Bollettino di Geofisica Teorica ed Applicata Vol. 60, n. 3, pp. 443-456; September 2019
DOI 10.4430/bgta0276

A statistical study of the M_W 5.3 Valandovo (northern Macedonia) earthquake seismic sequence

P. Raykova, D. Solakov and S. Simeonova

National Institute of Geophysics, Geodesy and Geography, Bulgarian Academy of Sciences, Sofia, Bulgaria

(Received: 10 December 2018; accepted: 21 March 2019)

ABSTRACT Studying of the space-time distribution of earthquakes is very important for understanding the physics of the earthquake generation process. The 2009 Valandovo earthquake, northern Macedonia, with moment magnitude M_W 5.3, was preceded by a foreshock sequence and followed by an intensive aftershock activity. We analyse the space-temporal pattern of earthquake distribution in the foreshock and aftershock sequences of the main event. We find short-distance clustering in both the pre-shock and aftershock period. The temporal distribution of foreshocks shows non-random features. Although dominated by the classic power law decay in time, the aftershocks suggest the existence of secondary aftershock sequence.

Key words: seismicity, foreshock, aftershock, northern Macedonia, Bulgaria, Greece.

1. Introduction

The spatial and temporal clustering of foreshocks and aftershocks is a dominant non-random element of the seismicity, so when the clusters are removed, the remaining activity can be modelled (as first approximation) as a Poisson process (Gardner and Knopoff, 1974). A formal definition of seismic clusters is still lacking despite of the conception that the earthquake clustering is an essential aspect of seismicity that provides key information on earthquake dynamics (Zaliapin and Ben-Zion, 2013). Statistically significant clusters consist of foreshocks, main-shocks, and aftershocks.

Foreshocks are one of the few well-documented precursors of large earthquakes. This type of sequences is observed within a few hours, several months or a year before the main shock (among others Molchan *et al*., 1999; Papadopoulos *et al*., 2000). Even if it is not considered a prognostic sign, the foreshocks show stress accumulation in the surroundings before the large earthquake. Therefore, understanding their nature is very important for earthquake prediction.

Aftershocks, on the other hand, are defined as seismicity above the background activity following a main shock (Liu and Stein, 2011). Aftershocks occur after the main event and their frequency decays over time, typically following a pattern known as the Omori's law, which later is modified by Utsu (1961) and is known as modified Omori's law. The power-low decay represented by the modified Omori relation is an example of temporal self-similarity of the earthquake source process. Aftershock decay rate may contain information about the mechanisms of stress relaxation and frictional strength heterogeneity (Mikumo and Miyatake,

1979) but this information cannot be derived without precise characterisation of the empirical relations that best fit the data. The duration of aftershock sequences may last months, a few years, or even longer for earthquakes within stable continental interiors (Stein and Liu, 2009). Some authors recognise that the main causes of aftershocks include main shock-induced changes of frictional properties of the fault zone and stress perturbations (e.g. Liu and Stein, 2011).

In the present study we examine the space-temporal pattern of foreshock and aftershock sequences of the 24 May 2009 earthquake with moment magnitude M_W 5.3 (T_0=16:17:49, φ=41.32°, λ=22.70° and h=5 km). The earthquake is reported by NOTSSI (Bulgarian Seismological Network) and ISC (International Seismological Centre) with body P-wave magnitude M_P=5.2 and surface-wave magnitude M_S=4.9, respectively. The event occurred in Valandovo seismogenic zone, situated in northern Macedonia, close to Bulgaria-Greece border region. The seismic zone is characterised by shallow intraplate seismicity. The strongest known event in the region is the 1931 Valandovo earthquake, with surface wave magnitude M_S=6.7 and epicentral intensity I_0=10 MSK. The event was preceded by a strong foreshock (with M_S=6.1, occurred a day before the main shock) and followed by intensive aftershock activity (Simeonova, 1999).

The manifold purpose of our study is first to examine spatial and temporal pattern of fore-aftershock distribution in the epicentral zone of the 2009 Valandovo earthquake (M_W 5.3), then to test different statistical models for aftershock occurrence based on the transformation of the time scale t to a frequency-linearised time scale τ. Finally, the Akaike Information Criterion [*AIC* (Akaike, 1974)] is used to select the best statistical model for aftershock occurrence.

2. Method and data

2.1. Method

For the aftershock data, we used the model obeying the modified Omori's law (Utsu, 1969):

$$n(t) = K(t+c)^{-p}, \tag{1}$$

where *n(t)* is frequency of aftershocks at time *t*; *t* is the elapsed time since the occurrence of the main shock, and *K*, *p*, *c* are constants. The most important parameter is the parameter *p*, which characterises the decay of the aftershock activity.

Based on the assumption that aftershocks are distributed as a non-stationary Poisson process, Ogata (1983) proposed to use the maximum likelihood method for estimating the parameters *K*, *c* and *p* in the modified Omori formula.

The intensity function of the Poisson process *l(t)* is defined by the relation:

$$\lambda(t) = \lim_{\Delta \to 0} Prob\{an\ event\ in\ [t, t+\Delta t]\} / \Delta t \ . \tag{2}$$

Then the likelihood function of the aftershock sequence can be as follows:

$$f(t_1, t_2, t_n, \theta) = \prod_{i=1}^{N} \lambda(t_i; \theta) exp(\int_S^T \lambda(t; \theta) dt), \tag{3}$$

where the t_i {i=1, 2, ... , N} are the occurrence times of the events in the available period of observation [S, T] and the corresponding vector θ is θ =(K, p, c).

Using the modified Omori formula, the intensity function becomes:

$$\lambda(t,\theta) = K\ (t\ +\ c)^{-p}\ . \tag{4}$$

If the sequence contains m secondary aftershock sequences, starting at times T_1, T_2, .., T_m, then the intensity function can be given as:

$$\lambda(t;\theta)\ =\ K(t+c)^{-p} + \sum\nolimits_{I=1} H(t-T_i)K_i(t-T_i+c_i)^{-pi}, \tag{5}$$

where H is the Heaviside unit step function and θ=(K, p, c, K_1, p_1, c_1, .., K_m, p_m, c_m).

The maximum likelihood estimates of the parameters are those, which maximise Eq. 4 with the corresponding vector θ (Ogata, 1983).

An integration of the intensity function $\lambda(t)$ gives a transformation from the time scale t to a frequency-linearised time scale τ (Ogata and Shimazaki, 1984). On this time axis the occurrence of aftershocks becomes the standard stationary Poisson process if the choice of the intensity function $\lambda(t)$ (i.e. the parameters K, c and p) is correct.

The frequency-linearised time for an aftershock sequence can be defined as:

$$\tau = \Lambda(t) = \int_0^t \lambda(s)ds \tag{6}$$

The time scale τ is used for testing the goodness of fit between the aftershock occurrence and the selected model. A linear dependence between the observed cumulative numbers of aftershocks N and τ should be observed if an appropriate model has been selected. Anomalies in the aftershock activity are more evident on the $N(\tau)$ plot than on $n(t)$. Thus, the τ time axis will be used to detect secondary aftershock activity.

In order to select which model fits the observations better, the *AIC* (Akaike, 1974) is used. This is a measure of which model most frequently reproduces features similar to the given observations, and is defined by:

$$AIC = (-2)\ Max\ (ln - likelihood) + 2\ (Number\ of\ the\ used\ parameters). \tag{7}$$

2.2. Input data

We have selected a space-time window in order to form the data set used in this study. All events recorded by NOTSSI that are located in the vicinity of the inferred rupture zone of the 2009 Valandovo earthquake are included. To define time boundaries, we study the frequency-time distribution of the earthquakes located in the considered area from May 2008 to December 2013 (Fig. 1).

The data show increasing rate of the seismic activity in the region in May 2009 and stayed relatively high for about 3 years (Fig. 1). The events in the area of Valandovo are almost uniformly distributed in time before May 2009 and after June 2012. Thus, the data we used for this study were earthquakes located in the area of Valandovo from 24 April 2009 to 24 June 2012. Since good azimuthal station coverage is required for accurate earthquake

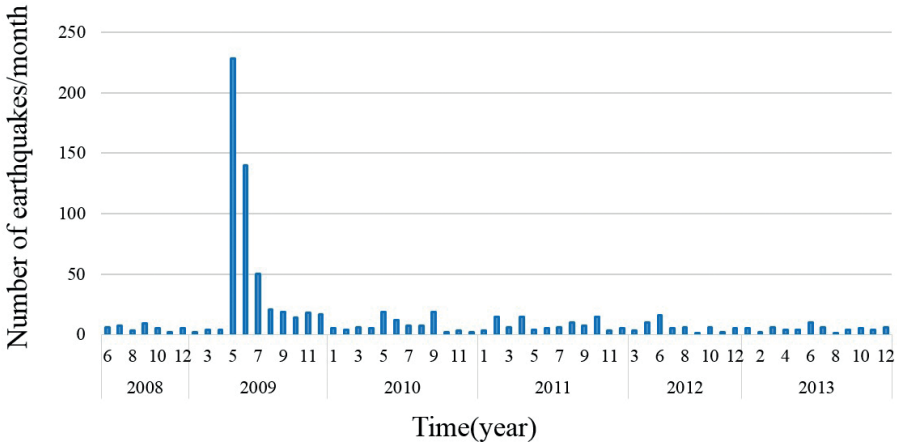

Fig. 1 - Frequency-time distribution for the earthquakes in the area of the Valandovo sequence.

location, we used additionally data from the local seismic networks in northern Macedonia, Greece, and Albania. To assure a consistency in the locations, we relocated all event for the sequence, applying a version of the HYPO 71 software called DHYPO (Solakov and Dobrev, 1987) which is used in the seismic location practice in NOTSSI. The body P-wave magnitude M_P after Christoskov *et al*. (2012) using the maximum amplitudes of body P waves of local earthquakes (up to 10°), recorded on the broadband seismographs, was estimated for each event of the compiled data set. To test the completeness of the events located in the selected area the magnitude frequency distribution is used (Fig. 2). The distribution indicates that the compiled data set is incomplete below M_P=2.0.

The data set is divided into two subsets: foreshocks (quakes preceding the main event) and aftershocks (earthquakes following the main event) and we are going to analyse them separately in the present study.

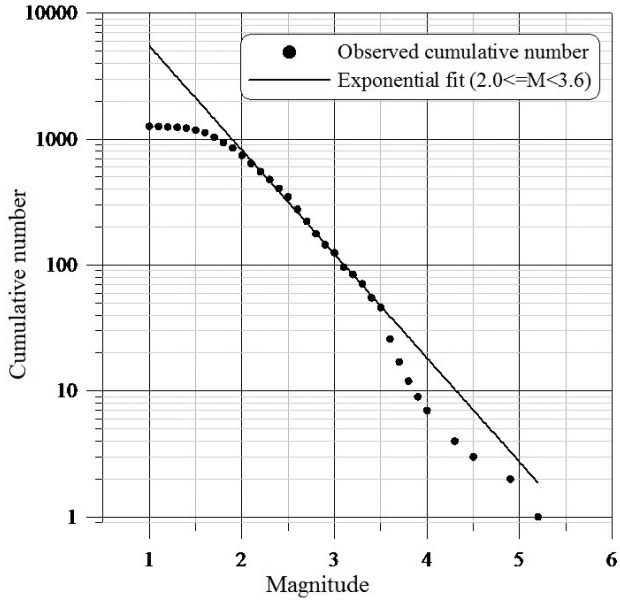

Fig. 2 - The magnitude frequency distribution.

We accept that aftershocks satisfy the space-time criteria introduced by Gardner and Knopoff (1974) and modified by Christoskov and Lazarov (1981) for the central Balkans:

$$\begin{aligned} &log\ R_a\ (M_m) = 0.9696 + 0.1243\ M_m \\ &log\ T_a\ (M_m) = -0.62 + 0.56\ M_m \qquad (M_m<6.0) \\ &log\ T_a\ (M_m) = -5.25 + 2.15\ M_m - 0.137\ M_m^2 \quad (M_m<6.0), \end{aligned} \tag{8}$$

where M_m is the surface-wave magnitude of the main event, R_a is the largest distance between the main event and an aftershock, and T_a is the greatest elapsed time since the occurrence of the main shock.

The map of epicentres is shown in Fig. 3, where foreshocks and aftershocks with M_P<4.0 are plotted as circles in yellow and green, respectively. The size of the circles is magnitude, M_P dependent (as presented in the legend). The strongest fore-aftershocks are plotted as asterisks in yellow and green, respectively. The dark red asterisk marks the main shock. The identified faults [modified from the neotectonic map in Ivanov *et al*. (2008)] are denoted by dark red lines. The area selected for the analysis in this paper is marked with a black square contour. The square is a side length of 2×R_a km, where R_a is defined using Eq. 8. Since the main event has a surface-wave magnitude of M_S=4.9 (reported by ISC) and the estimated R_a is 37.9 km, the square side is about 76 km. In the present study, we consider only earthquakes with epicentres falling inside this area.

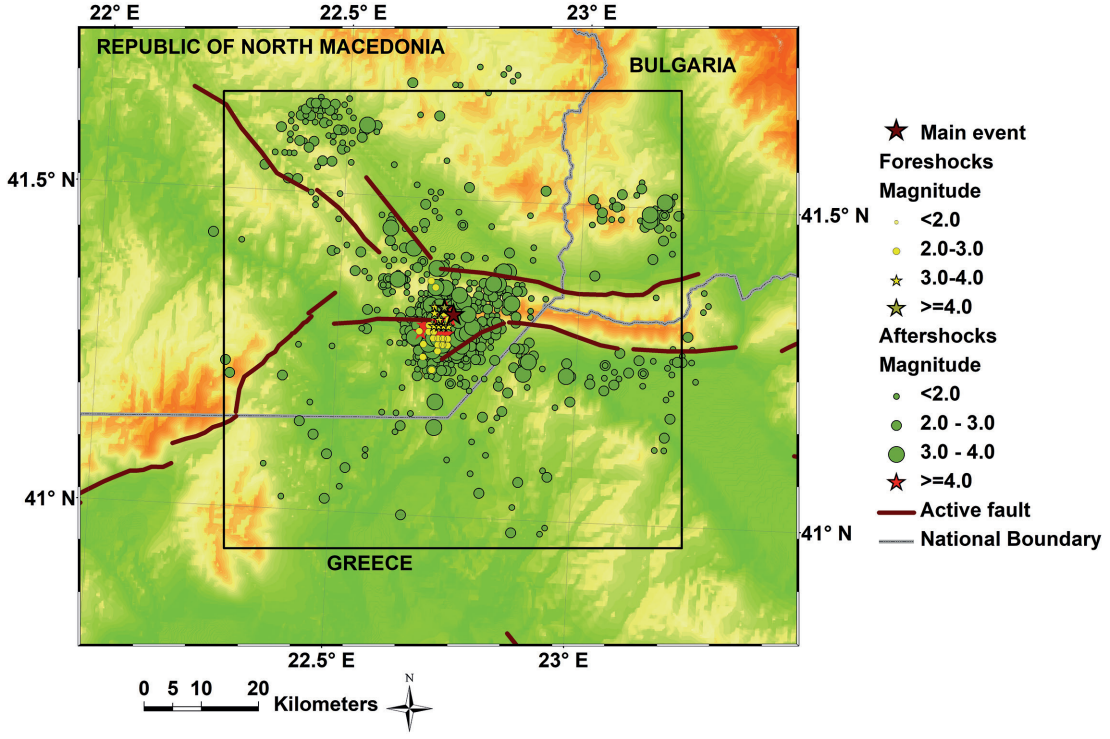

Fig. 3 - Epicentral map of the earthquakes located in the selected area occurred between 23 April 2009 and 24 May 2012.

3. Results

The results of the present study are presented in Figs. 3 to 11 and Table 1. The spatial distribution of earthquakes in the considered sequence is shown in Figs. 3 to 7. The temporal distribution of foreshocks and aftershocks is presented in Figs. 8 to 11 and Table 1.

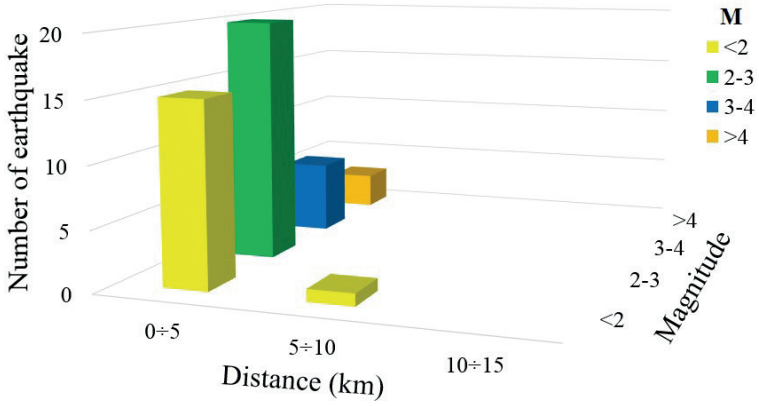

Fig. 4 - Distribution of distances between the main event and foreshocks.

3.1. Spatial distribution

The spatial distribution of pre-shocks is presented in Figs. 3 and 4. The figures illustrate the epicentral map (Fig. 3) and distribution of distances to the main shock (Fig. 4) for foreshocks, which, occurred within the selected area (black contour in Fig. 3).

Both figures display non-random features that can be summarised as follows: 1) foreshocks are clustered in a small area between the identified fault structures (Fig. 3); 2) the main shock occurred on the fault located in the foreshocks area margin (Fig. 3); 3) an excessive number of earthquakes is observed for distances ≤ 5 km (Fig. 4).

The aftershock data are split in early aftershocks considered in two time periods: one month and one year after the main event, and all aftershocks (from 24 May 2009 to 24 May 2012). The division of the aftershock data set is based on the assumption that if several data sets share a common, weak pattern, then their joint study may make the pattern detectable. While if the pattern is not common for all of the sets, it may be masked (Eneva and Pavlis, 1988).

Plots of panel a of Figs. 5 to 7 illustrate the spatial distribution of aftershocks for the time periods of 31 days, 364 days, and 1092 days after the 2009 Valandovo earthquake, respectively. Plots of panel b of the same Figs. 5 to 7 show the main event to aftershock distance distribution for the same time periods.

The joint study of the three data sets make the following characteristics in the aftershock spatial patterns more detectable: 1) the main shock and aftershocks in the first 31 days are clustering in the area outlined by the foreshocks, between three fault structures (Fig. 5a); 2) a well-expressed tendency of aftershock area expansion in time and with decrease of magnitude (Figs. 6a and 7a); 3) the aftershocks with magnitude M_p<3.0 are dispersed in space and spread over a large area (Fig. 7a); 4) concentration of earthquakes in three clusters, separated by distance gaps (Fig. 7a); 5) an excess of events separated by distances larger than 20 km is

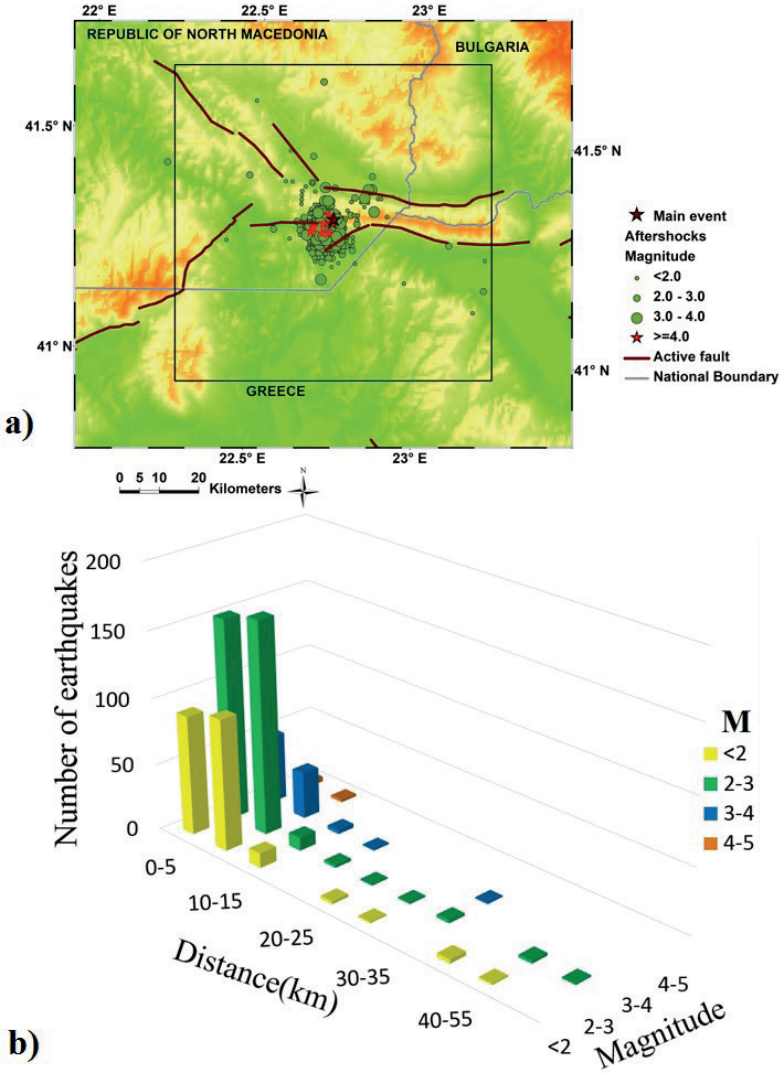

Fig. 5 - Epicentral map and spatial distribution for early aftershocks (time period: 24 May 2009 to 24 June 2009).

observed in the later stage of the aftershock sequence (Fig. 7); 6) most of the largest aftershocks are clustered along the E-W extending fault (Figs. 5a and 7a); 7) larger events tend to be more clustered than smaller ones (Figs. 5b and 7b).

3.2. Temporal distribution

The foreshock temporal distribution is shown in Fig. 8 and indicates that the pre-shocks have an uneven distribution over time. A well-expressed cluster occurred approximately 24 hours before the main event (Fig. 8a). Two clusters separated by a gap of 6 hours and no precursor aseismic gap before the main shock are observed in Fig. 8b.

We analyse the aftershock sequence from 0 to T_a=133 days after the main earthquake. The time interval T_a is the calculated value of the greatest elapsed time since the occurrence of the main shock using Eq. 8. In the study, two sets of data are analysed: the first includes all aftershocks, located inside the box shown in Fig. 3; the second data set covers all events with magnitude M_L≥2.0, located inside the area of interest. The reason to separate aftershocks into

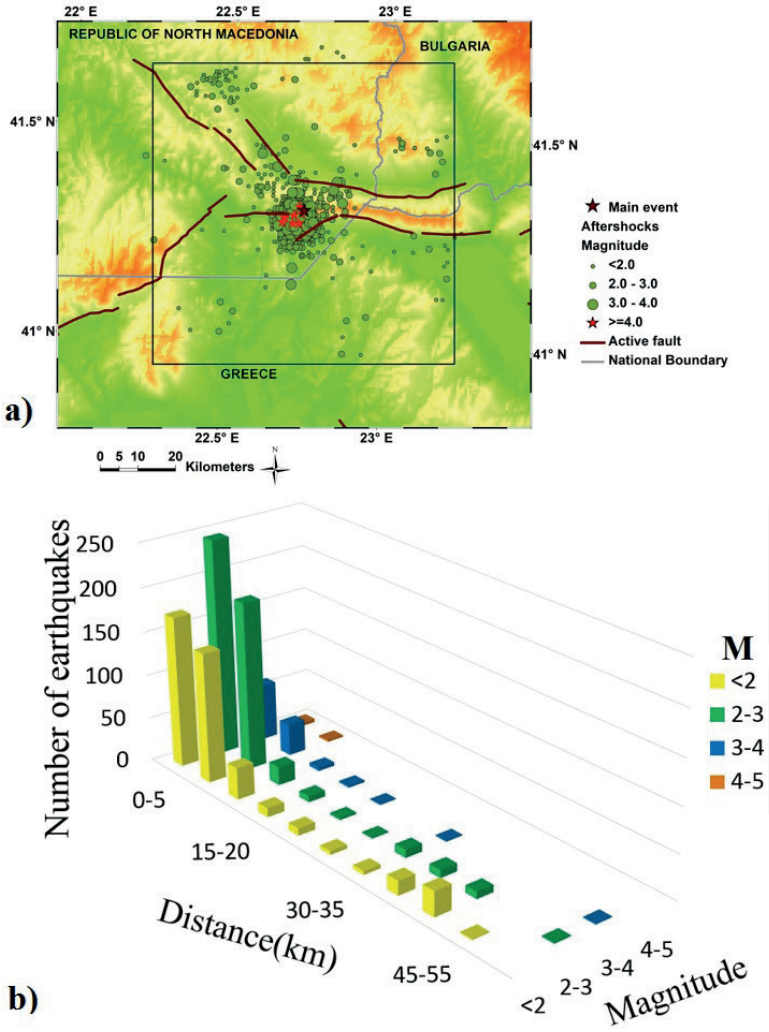

Fig. 6 - Epicentral map and spatial distribution for early aftershocks (time period: 24 May 2009 to 24 May 2010).

two data sets is that the catalogue is incomplete below the magnitude M_p<2.0, as inferred from the magnitude-frequency relationship (Fig. 2) for the events in the area of Valandovo.

The parameters K, c, and p in the modified Omori formula (Eq. 1) are estimated using the maximum likelihood method. The estimated values for these parameters are presented in Table 1. The frequency-time distributions of earthquakes are presented in Fig. 9.

The cumulative number of events is plotted against the frequency-linearised time τ, (as defined in Eq. 6) using the estimated parameters K, p, c (Fig. 10). The observed distribution is compared to the theoretical distribution, based on the selected model (in this case, the model is the modified Omori formula). If the modelling of the sequence is appropriate, the cumulative number of events will increase linearly with τ. There is a relatively good correlation between the theoretical and the observed distribution for both analysed cases.

Fig. 10 shows bumps about 8 days after the main shock in both plots. The aftershock activity decreases around the 8th day and increases after it. This temporal distribution anomaly could be caused by the occurrence of one of the strongest aftershocks on 1 June 2009 with magnitude M_p4.3.

Consequently, we reconstructed a model, which takes into account the effect of a secondary

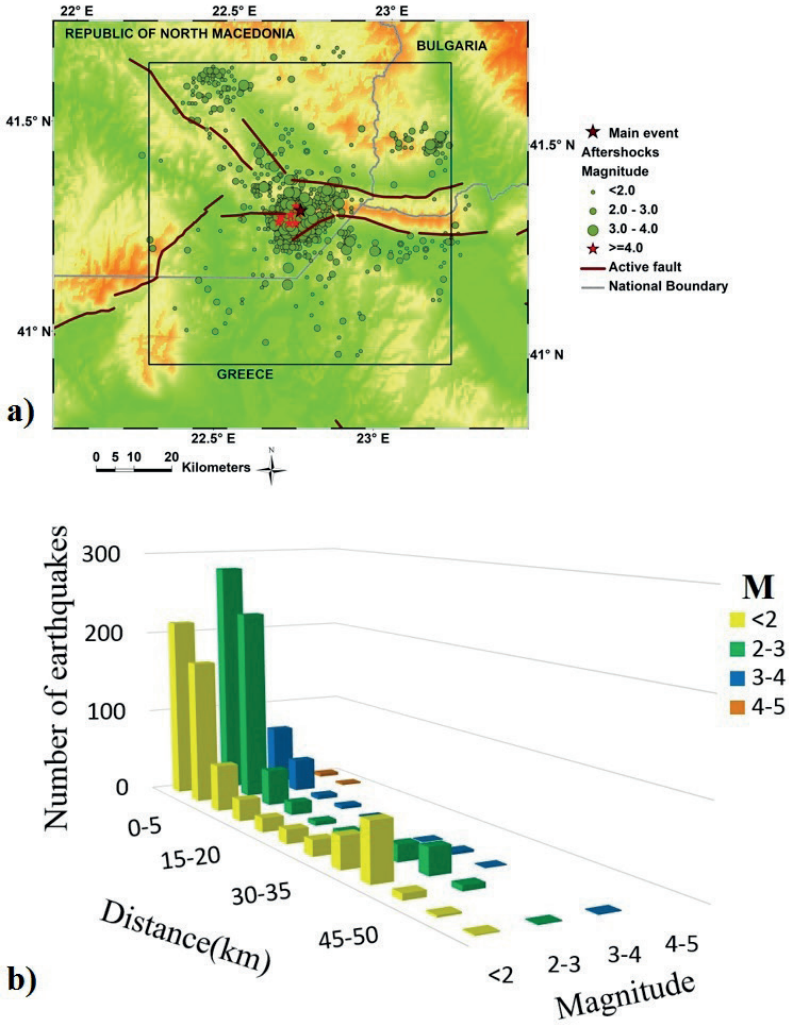

Fig. 7 - Epicentral map and spatial distribution for all aftershocks that occurred in the area selected for analysis from 23 April 2009 to 24 May 2012.

aftershock activity. We tested a model with one secondary aftershock sequence after 8 days and the same p value for the main and secondary aftershock sequences. The model is applied for the two data sets.

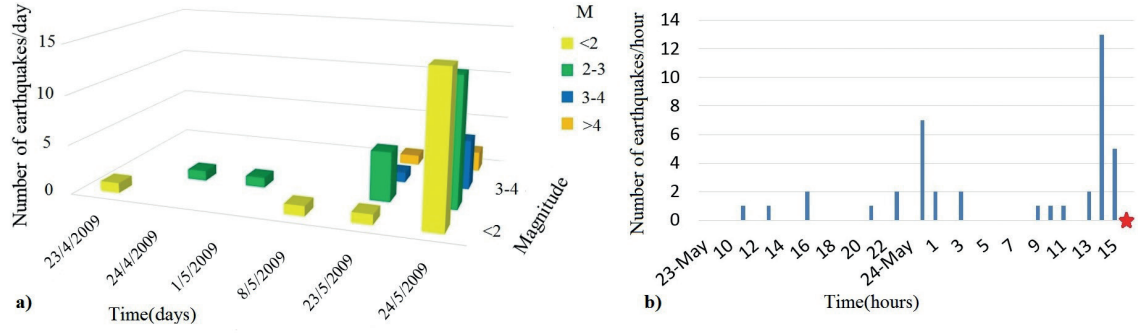

Fig. 8 - Temporal distribution of foreshocks: a) distribution of pre-shocks in days; b) hourly distribution of foreshocks before the main event (red star).

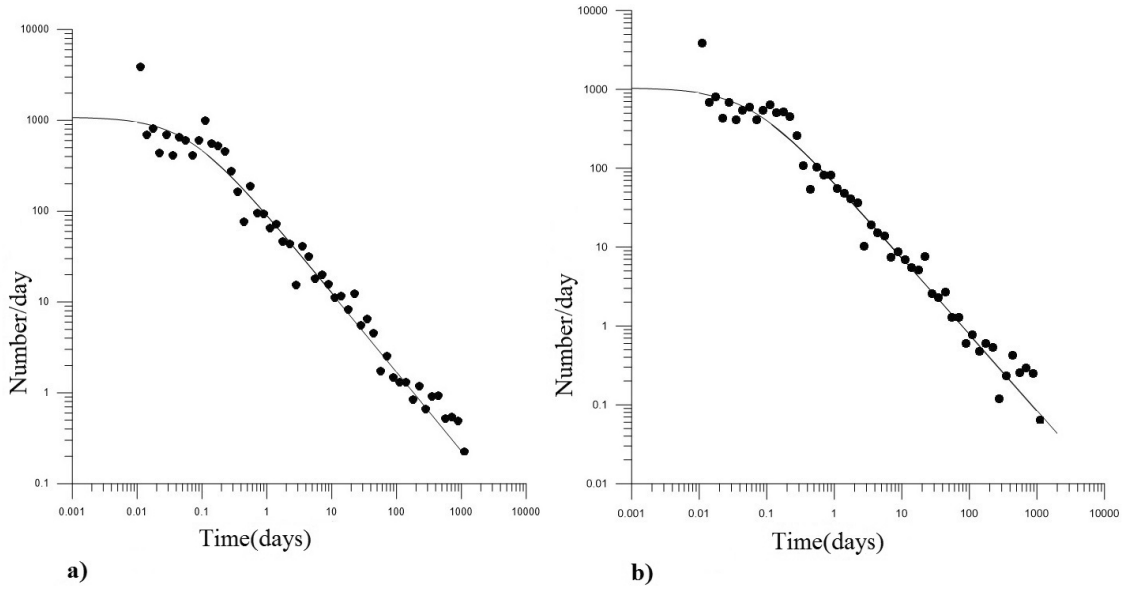

Fig. 9 - Frequency-time distributions of aftershocks: a) for a set of data including all aftershocks; b) aftershocks with magnitude $M_P \geq 2.0$.

The results (Fig. 11 and Table 1) show that the model with one ordinary and one secondary sequence describes best the aftershock sequence of the 2009 earthquake. We can see a good fit between observed and expected distributions without evident periods of decaying and activation of the process.

Fig. 11 shows that a nearly-linear trend of aftershock decay continues up to 647 days. Thus, the modified Omori formula (Eq. 1) fits the observations up to 647 days after the main shock. About 647 days after the main shock the cumulative number of aftershocks increases rapidly

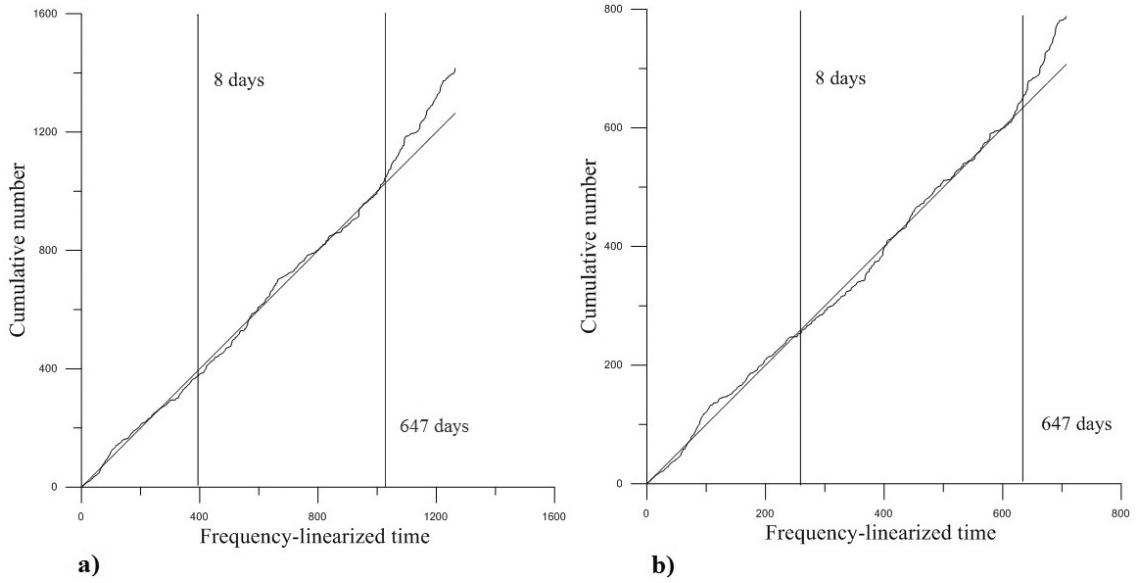

Fig. 10 - Plot of the cumulative number of events versus frequency-linearised time τ: a) all aftershocks; b) aftershocks with magnitude $M_P \geq 2.0$.

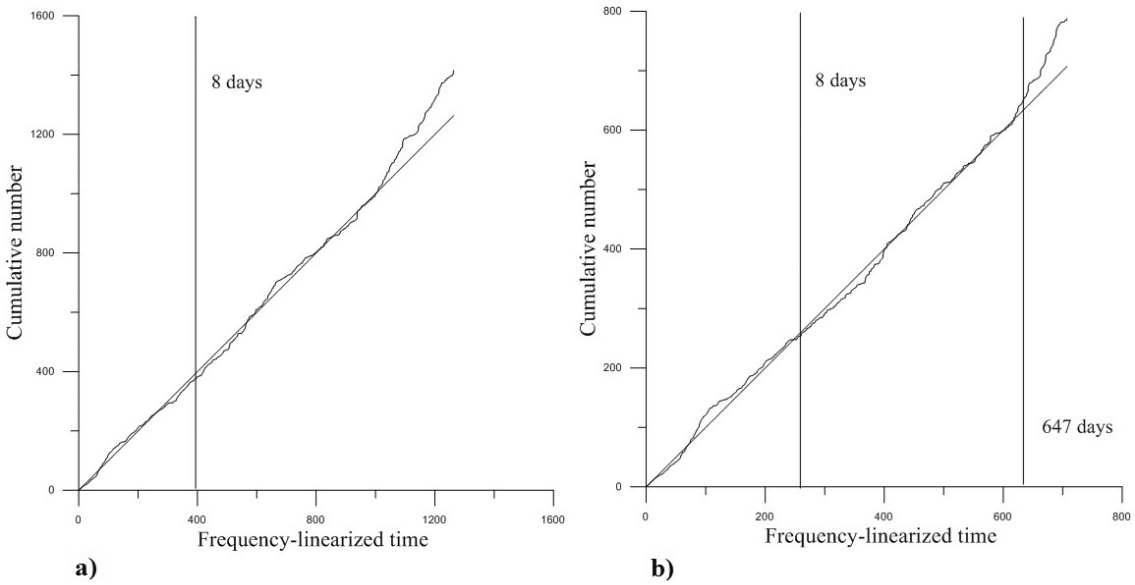

Fig. 11 - Plot of the cumulative number of events versus frequency-linearised time τ for the 2009 aftershock sequence for an ordinary and one secondary aftershock: a) for all aftershocks; b) for aftershocks with magnitude $M_L \geq 2.0$.

Table 1 - Maximum likelihood estimates of the Omori formula parameters and corresponding AIC.

Model	*K*	*P*	*c*	K_1	p_1	c_1	*AIC*
An ordinary aftershock sequence, without threshold magnitude	93.69	0.87	0.06				-3559.64
One ordinary and one secondary aftershock sequences, without threshold magnitude	92.71	0.88	0.06	1.02	0.88	0.0002	-3569.59
An ordinary aftershock sequence, with threshold magnitude M_a=2	68.00	0.97	0.06				-2254.27
One ordinary and one secondary aftershock sequences, with threshold magnitude M_a=2	67.61	0.97	0.06	0.47	0.97	0.0034	-2255.21

with τ, showing a significant deviation from the prior trend. No large earthquake occurred in the region at that time. Therefore, this change in slope could be treated as a transition from aftershock activity to background seismicity. It should be noted that the predicted duration of the aftershock activity is 133 days (by Eq. 9) and is approximately 4.8 times less than the observed duration.

4. Discussion and conclusions

The prime result of our paper is the discovery that the space - temporal distribution of earthquakes in the Valandovo region was non-uniform both before and after the main event on 24 May 2009. The analysis performed allows us to see that when a non-random feature is present, it is manifested as a function of space, time and magnitude.

Spatial clustering is observed both before and after the main shock. The larger the events, the higher the degree of clustering is observed. Foreshocks are clustered in a very small area at 2 to 10 km from the main shock. The epicentral maps (best seen in Fig. 3) indicate that the aftershocks appear to enhance an existing spatial pattern rather than create a new one. In addition, the clustering appears to increase with time, as a result of growth the average size of clusters and an increasing degree of non-randomness (compare Figs. 5a and 7a). We also observed an anomaly related to the lack of aftershocks between 11 km and 30 km from the main event epicentre (compare Figs. 6b and 7b). In fact, it appears later (about 1 year after the main earthquake) in the sequence and is associated with a concentration of earthquakes in three clusters, separated by distance gaps. This trend is due to occurrence of a substantial number of small earthquakes in parts of the fault zone that were virtually aseismic before the main shock (compare Figs. 6a and 7a). One possible interpretation of this observation could be based on the assumption that, during an aftershock sequence, small earthquakes occur as a consequence of the transient stress inhomogeneity within the fault zone caused by the main shock. If we associate the degree of spatial non-randomness in earthquake distribution with the degree of non-uniformity of stress in the area, an increased degree of clustering can, then, be related to an increased non-uniformity in stress.

The foreshock temporal distribution suggests significant non-random features. Two clusters divided by a gap of about 6 hours are observed. Furthermore, the main shock occurs several minutes after the second cluster. Aseismic time interval between the pre-shocks and the main event is not observed.

Our results show that the aftershock activity is best modelled by one ordinary and one secondary sequence. An objectively defined transition from aftershock activity to background seismicity is observed about 647 days after the main shock. It should be noted that the predicted duration of the aftershock activity is 133 days: approximately 4.8 times less than the observed duration.

Aftershock decay rate (parameter p in modified Omori's law) contains information about the mechanisms of stress relaxation and frictional strength heterogeneity (Mikumo and Miyatake, 1979). The variability in the values of the characteristic p-value is related to the structural heterogeneity, stress and temperature in the crust (Mogi, 1962; Kisslinger and Jones, 1991). During the last years, more than 200 estimates of p-value with a scatter from 0.6 to 2.5 and a median of 1.1, have been published for aftershock sequences in different parts of the world (Utsu *et al*., 1995). The p-value estimate in the present study is in the middle of the p-value range obtained for aftershock sequences in Bulgaria and surroundings, $0.71 \leq p \leq 1.17$ (Simeonova and Solakov, 1999) and it is the lower part of interval obtained for aftershock sequences in Greece, i.e. $0.83 \leq p \leq 1.86$ (Papazachos, 1975).

The findings of our study are consistent with a number of papers [among others Simeonova (1999), Simeonova *et al*. (2015), Solakov *et al*. (2016) and Raykova (2017)] which suggest that non-uniformity in space-temporal distribution of fore-aftershocks is an intrinsic feature of earthquake occurrence in Bulgaria and the surrounding regions.

Finally, if we accept the following two assumptions: 1) examination of the space-time distribution of earthquakes is of fundamental importance for understanding the physics of earthquake generation process [among others Eneva and Pavlis (1988)]; and 2) the earthquake generation is an expression of the regional tectonics; then the results from this study of the 2009 M_W 5.3 Valandovo earthquake seismic sequence could be interpreted as a confirmation of the

hypothesis that the neotectonic movements of southern Bulgaria and the surroundings (in our case eastern part of northern Macedonia) are similar to that of northern Greece and the northern Aegean Sea with presently N-S extension [among others van Eck and Stoyanov (1996)].

We can summarise our principal findings from the study of the Valandovo earthquake sequence as follows:

1. the spatial distribution of earthquakes is not uniform either before or after the main shock on 24 May 2009;
2. clustering of earthquakes is observed both before and after the main shock. Foreshocks are concentrated in a relatively small area within the identified fault structures where, later, the main shock and the strongest aftershocks occurred. The observed pattern is intensified in the aftershock sequence because of an increase in the size of cluster with time. Larger events tend to be more clustered than smaller ones;
3. a concentration of earthquakes is observed at a distance of less than 10 km from the main shock. This pattern exists before the main shock and in the first 31 days of the aftershock activity. An excess of events separated by distances larger than 20 km is also observed in the later stage of the aftershock sequence. It is associated with a concentration of earthquakes in three clusters, separated by distance gaps with a distinct reduced number of aftershocks;
4. the temporal distribution of foreshocks shows non-random features. 24 hours before the earthquake, two clusters separated by a gap of 6 hours and no precursor aseismic gap before the main shock are observed;
5. the 2009 M_W 5.3 earthquake aftershock sequence is best modelled by the combination of one ordinary and one secondary aftershock sequence. Transition from aftershock activity to background seismicity is observed about 647 days after the main shock.

Acknowledgements. The authors would like to thank the two anonymous reviewers for useful comments and improvements to the manuscript. During the work, Plamena Raykova is World Federation of Scientists grant holder.

REFERENCES

Akaike H.; 1974: *A new look at the statistical model identification*. IEEE Trans. Automatic Control AC-19, 716-723, doi: 10.1109/TAC.1974.1100705.

Christoskov L. and Lazarov R.; 1981: *General considerations on the representativeness of the seismological catalogues with a view to the seismostatistical investigations*. Bulg. Geoph. J., **3**, 58-72, (in Bulgarian).

Christoskov L., Dimitrova L. and Solakov D.; 2012: *Digital broadband seismometers of NOTSSI for practical magnitude determinations of P waves*. Comptes Rendus de L'Academie Bulgare des Sciences, **65**, 653-660.

Eneva M. and Pavlis G.; 1988: *Application of pair analysis statistics to aftershocks of the Morgan Hill, California*, earthquake. J. Geophys. Res., **93**, 9113-9125.

Gardner J.K. and Knopoff L.; 1974: *Is the sequence of earthquakes in southern California, with aftershocks removed Possionian?* Bull. Seismol. Soc. Am., **64**, 1363-1367.

Ivanov J., Nakov R., Gerdzikov Y. and Radulov A.; 2008: *Part 6 - Geology*. In: Report Geophys. Ist. - BAS, (fund NIGGG), Sofia, Bulgaria, pp. 80-113, (in Bulgarian).

Kisslinger C. and Jones L.; 1991: *Properties of aftershock sequences in southern California*. J. Geophys. Res., **96**, 11947-11958.

Liu M. and Stein, S.; 2011: *Aftershocks*. In: Gupta, H. (ed), Encyclopedia of Solid Earth Geophysics, Springer, Dordrecht, The Netherlands, pp. 192-194.

Mikumo T. and Miyatake T.; 1979: *Earthquake sequences on a frictional fault model with non-uniform strengths and relaxation times*. Geophys. J. R. Astr. Soc., **59**, 497-522.

Mogi K.; 1962: *Study of the elastic shocks caused by fracture of the heterogeneous materials and its relation to earthquake phenomena*. Bull. Earthquake Res. Inst. Univ. Tokyo, **49**, 125-173.

Molchan G.M., Kronrod T.L. and Nekrasona A.K.; 1999: *Immediate foreshocks: time variation of the b-value*. Phys. Earth Planet. Int., **111**, 229-240.

Ogata Y.; 1983: *Estimation of the parameters in the modified Omori formula for aftershock sequences by the maximum likelihood procedure*. J. Phys. Earth, **31**, 115-124.

Ogata Y. and Shimazaki K.; 1984: *Transition from aftershock to normal activity: the Rat Islands earthquake aftershock sequence*. Bull. Seismol. Soc. Am., **74**, 1757-1765.

Papadopoulos G.A., Drakatos G. and Plessa A.; 2000: *Foreshock activity as a precursor of strong earthquakes in Corinthos Gulf, Central Greece*. Phys. Chem. Earth, **25**, 239-245.

Papazachos B.C.; 1975: *On certain aftershock and foreshock parameters in the area of Greece*. Ann. Geofis., **28**, 497-515.

Raykova P.; 2017: *Characteristics of fore-aftershock and swarm type activity for Bulgaria and surroundings*. Ph.D. Thesis, NIGGG-BAS, Sofia, Bulgaria, 48 pp., (in Bulgarian).

Simeonova S.; 1999: *A study of the Central Balkans (Bulgaria and surroundings) aftershock sequences*. Ph.D. thesis, Geoph. Ist. - BAS, Sofia, Bulgaria, pp. 38, (in Bulgarian).

Simeonova S. and Solakov D.; 1999: *Temporal characteristics of some aftershock sequences in Bulgaria*. Ann. Geofis., **42**, 821-832.

Simeonova S., Solakov D., Aleksandrova I., Raykova P. and Protopopova V.; 2015: *The 2012 M_W 5.6 earthquake in Sofia seismic zone and some characteristics of the aftershock sequence*. Bulg. Chem. Comm., **47**, Spec. Issue B, 397-404.

Solakov D. and Dobrev Tch.; 1987: *Program for earthquake parameters determination*. Bulg. Geophys. J., **13**, 100-104, (in Bulgarian).

Solakov D., Simeonova S., Raykova P., Aleksandrova I., Popova M. and Protopopova V.; 2016: *Seismological analysis of the 2012 M_W 5.6 earthquake in Sofia Seismic Zone*. Comptes rendus de l'Acad´emie bulgare des sciences: sciences mathematique et naturelles, **69**, 67-74.

Stein S. and Liu M.; 2009: *Long aftershock sequences within continents and implications for earthquake hazard assessment*. Nature, **462**, 87-89.

Utsu T.; 1961: *A statistical study of the occurrence of aftershocks*. Geophys. Magaz., **30**, 521-605.

Utsu T.; 1969: *Aftershocks and earthquake statistics (I) - Some parameters which characterize an aftershock sequence and their interaction*. J. Fac. Sc., Hokaido Univ., Ser. VII (Geophys.), **3**, 129-195.

Utsu T., Ogata Y. and Matsu'ura R.; 1995: *The centenary of the Omori formula for a decay law of aftershock activity*. J. Phys. Earth, **43**, 1-33.

van Eck T. and Stoyanov T.; 1996: *Seismotectonics and seismic hazard modelling for southern Bulgaria*. Tectonophys., **262**, 77-100.

Zaliapin I. and Ben-Zion Y.; 2013: *Earthquake clusters in southern California I: Identification and stability*. J. Geophys. Res., Solid Earth, **118**, 2847-2864.

Corresponding author: Plamena Raykova
National Institute of Geophysics, Geodesy and Geography, Bulgarian Academy of Sciences
Acad. G. Bonchev str., Sofia 1113, Bulgaria
Phone: +359 888 092214; e-mail: plamena.raikova@gmail.com